Redistribution and activation of implanted S, Se, Te, Be, Mg, and C in GaN

R. G. Wilson
Consultant, Stevenson Ranch, California 91381

J. M. Zavada
U.S. Army, Research Office, Research Triangle Park, North Carolina 27709

X. A. Cao, R. K. Singh, and S. J. Pearton[a)]
Department of Materials Science and Engineering, University of Florida, Gainesville, Florida 32611

H. J. Guo and S. J. Pennycook
Solid State Division, Oak Ridge National Laboratory, Oak Ridge, Tennessee 37831

M. Fu, J. A. Sekhar, and V. Scarvepalli
Micropyretics Heaters International, Inc., Cincinnati, Ohio 45215

R. J. Shu, J. Han, and D. J. Rieger
Sandia National Laboratories, Albuquerque, New Mexico 87185

J. C. Zolper
Office of Naval Research, Arlington, Virginia 22217

C. R. Abernathy
Department of Materials Science and Engineering, University of Florida, Gainesville, Florida 32611

(Received 11 September 1998; accepted 30 November 1998)

A variety of different possible donor and acceptor impurities have been implanted into GaN and annealed up to 1450 °C. S^+ and Te^+ produce peak electron concentrations $\leqslant 5\times10^{18}$ cm^{-3}, well below that achievable with Si^+. Mg produces *p*-type conductivity, but Be^+- and C^+- implanted samples remained *n* type. No redistribution was observed for any of the implanted species for 1450 °C annealing. Much more effective damage removal was achieved for 1400 °C annealing of high-dose (5×10^{15} cm^{-2}) Si^+ implanted GaN, compared to the more commonly used 1100 °C annealing. © *1999 American Vacuum Society.* [S0734-2101(99)01404-9]

I. INTRODUCTION

Ion implantation is the preferred method for selected-area doping of semiconductors due to its high spatial and dose control and its high throughput capability.[1–10] In GaN there have been a number of systematic reports detailing the achievement of *n*- and *p*-type doping[11–15] (using Si and O for *n* type, and Mg and Ca for *p* type) and the application of ion implantation to improving ohmic contact resistance on heterostructure field-effect transistors,[16] and to producing *p*-*n* junctions for fabrication of junction field-effect transistors[12] and for light-emitting diodes.[4] At high implant doses ($\geqslant 5\times10^{14}$ cm^{-2}) it is clear that conventional rapid thermal annealing (RTA) at 1100–1200 °C can activate the dopants but not remove the ion-induced structural damage.[14,15] At higher annealing temperatures ($\geqslant$1400 °C), it is difficult to provide a sufficiently high N_2 pressure to prevent dissociation of the GaN surface. Three different approaches have been reported: the first is use of an NH_3 ambient in a metalorganic chemical vapor deposition (MOCVD) reactor,[17] the second is use of a high N_2 overpressure (15 kbar) in a GaN bulk crystal growth apparatus,[14] and the third is use of an AlN encapsulant to prevent nitrogen loss from the GaN.[18] The third approach is clearly the most convenient.

What is needed is a better understanding of the optimum dopants for creation of *n*- and *p*-type regions in GaN, based on the highest achievable electron or hole concentrations, the residual damage and the redistribution during high temperature annealing. Currently, the only information of this type available is for Si (a donor) and Mg (an acceptor). In this article, we report on the high temperature activation characteristics of two alternative donor implant species, S and Te, which do not have the potential drawback of being amphoteric like Si in GaN. The activation characteristics of Mg and C for *p*-type doping have also been examined, along with the redistribution of all these species plus Se and Be. Finally, the efficiency of high temperature RTA for removing lattice damage in implanted GaN was examined by transmission electron microscopy (TEM). In all cases we compare the results with those for Si, the standard implant species for *n*-GaN.

II. EXPERIMENT

Nominally undoped ($n\sim5\times10^{16}$ cm^{-3}) GaN was grown on *c*-plane Al_2O_3 substrates at 1040 °C by MOCVD using triethylgallium and ammonia. Samples were implanted at room temperature in a nonchanneling direction with 80 keV $^{9}Be^+$, 80 keV $^{12}C^+$, or 150 keV $^{24}Mg^+$ for *p*-type doping, or with 150 keV $^{28}Si^+$, 200 keV $^{32}S^+$, 300 keV $^{80}Se^+$, or 600 keV $^{128}Te^+$ ions for *n*-type doping, at doses of $3-5\times10^{14}$ cm^{-2}. Additional samples had previously been im-

[a)]Electronic mail: spear@mse.ufl.edu

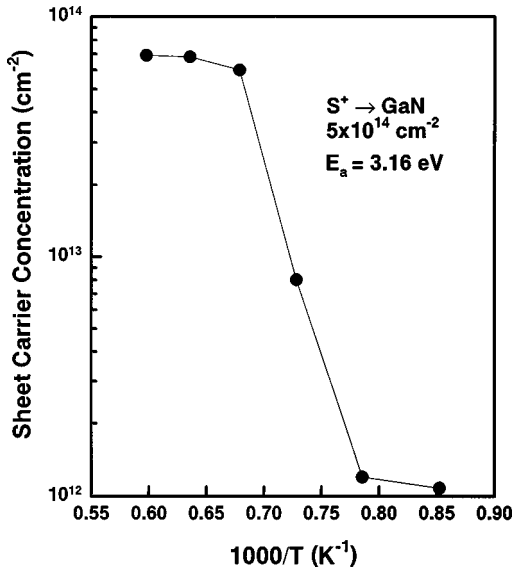

FIG. 1. Arrhenius plot of sheet electron density in S^+-implanted GaN vs annealing temperature.

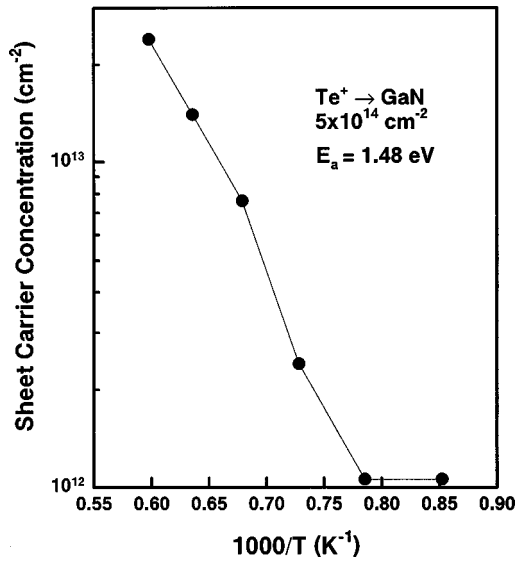

FIG. 2. Arrhenius plot of sheet electron density in Te^+-implanted GaN vs annealing temperature.

planted with 150 keV $^{28}Si^+$ ions at a dose of 5×10^{15} cm^{-2}—this is a standard condition for producing very high *n*-type doped regions in GaN when combined with high temperature RTA.[17] All samples were capped with ~1000 Å reactively sputtered AlN, and annealed at 1200–1500 °C under a N_2 ambient in the Zapper™ furnace for a dwell time of ~10 s.[19] Following annealing, the AlN was removed in aqueous KOH at ~80 °C, and the samples were characterized. For measurement of the electrical properties, HgIn ohmic contacts were alloyed to the corners of 3×3 mm^2 sections, and Hall effect data were recorded at 25 °C in all cases. Finally, some of the Si-implanted samples were examined by plan-view TEM, since Si remains the standard implant species for GaN *n*-type doping, and it has a representative mass number that allows comparison to damage expected with S, Ca, and Mg.

III. RESULTS AND DISCUSSION

A. Dopant activation

Figure 1 shows an Arrhenius plot of S^+ activation in GaN. The sheet carrier concentration measured at 25 °C shows an activation energy of 3.16 eV for the annealing temperature range between 1000 and 1200 °C and basically saturates thereafter. The maximum sheet electron density, $\sim7\times10^{13}$ cm^2, corresponds to a peak volume density of $\sim5\times10^{18}$ cm^{-3}. This is well below that achieved with Si^+ implantation and annealing ($>10^{20}$ cm^{-3}).[17,20] In the latter case, the carrier density showed an activation energy of 5.2 eV. The physical origin of this activation energy contains several components—basically it is the energy required to move an implanted ion onto a substitutional lattice site and for it to show electrical activity. This latter requirement means that compensating defects must also be annealed out. Even though implanted Si^+ at the same dose showed evidence of site switching and self compensation, it still produces a higher peak doping level than the nonamphoteric donor S, which is only slightly heavier (^{32}S vs ^{28}Si). From temperature-dependant Hall measurements, we find a S^+ donor ionization level of 48±10 meV, so that the donors are fully ionized at room temperature.

Similar data is shown in Fig. 2 for Te^+ implantation. The activation starts around the same temperature as for S, but much lower sheet electron densities are obtained, the activation energy is significantly lower (1.5 eV) and the carrier concentration does not saturate, even at 1400 °C. It is likely that because of the much greater atomic weight of ^{128}Te, even higher annealing temperatures would be required to remove all its associated lattice damage, and that the activation characteristics are still being dominated by this defect removal process. Residual lattice damage from the implantation is electrically active in all III–V semiconductors, producing either high resistance behaviors (GaAs) or residual *n*-type conductivity (InP, GaN). The only data available on group VI doping in epitaxial material are from Se-doped MOCVD material, where maximum electron concentrations of 2×10^{18}–6×10^{19} cm^{-3} were achieved.[21,22] These are also below the values reported for Si doping, and suggests the group VI donors do not have any advantage over Si for creation of *n*-type layers in GaN. From limited temperature-dependent Hall data, we estimate the Te ionization level to be 50±20 meV.

The effects of post-implant annealing temperature on the sheet carrier concentrations in Mg^+ and C^+ implanted GaN are shown in Fig. 3. There are two important features of the data: first, we did not achieve *p*-type conductivity with carbon, and second only ~1% of the Mg produces a hole at 25 °C. Carbon has been predicted previously to have a strong self-compensation effect,[23] and it has been found to produce *p*-type conductivity only in metalorganic molecular beam epitaxy where its incorporation on a N-site is favorable.[24] Based on an ionization level of ~170 meV, the hole density

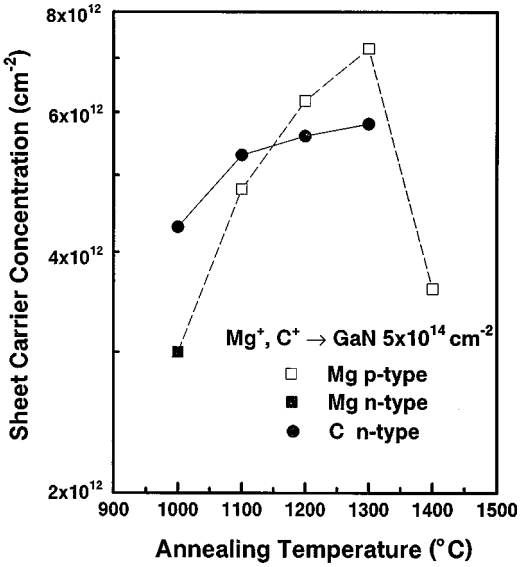

FIG. 3. Sheet carrier densities in Mg^+- or C^+-implanted GaN as a function of annealing temperature.

in Mg-doped GaN would be calculated to be ~10% of the Mg acceptor concentration when measured at 25 °C. In our case, we see an order of magnitude less holes than predicted. This should be related to the existing *n*-type carrier background in the material and perhaps to residual lattice damage which is also n-type in GaN, At the highest annealing temperature (1400 °C), the hole density falls, which could be due to Mg coming out of the solution or to the creation of further compensating defects in the GaN.

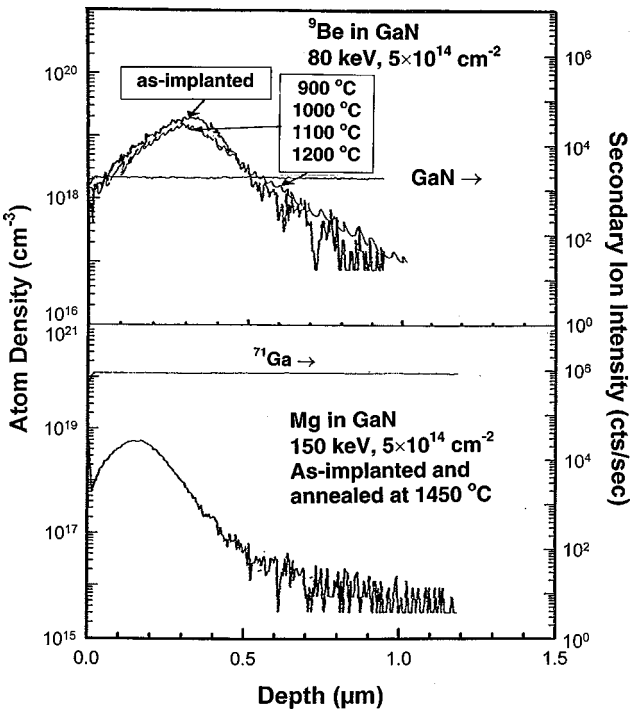

FIG. 4. SIMS profiles of Be^+- and Mg^+-implanted into GaN as a function of annealing temperature.

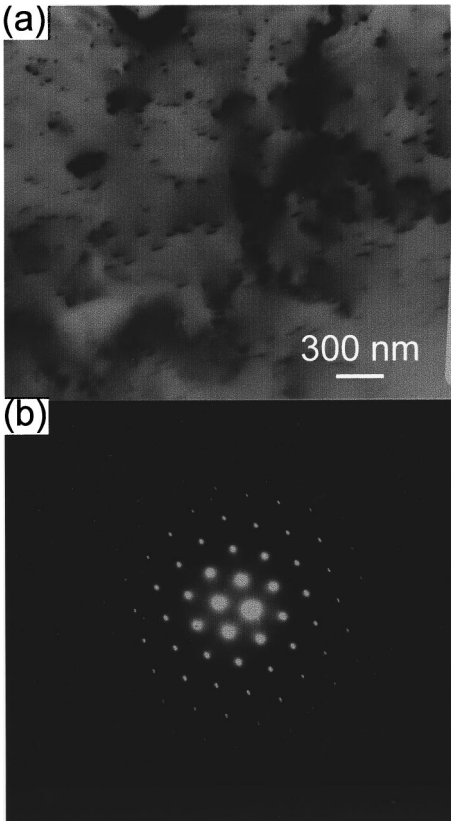

FIG. 5. (a) TEM plan view and (b) selected-area diffraction pattern from Si^+-implanted GaN (5×10^{15} cm^{-2}, 150 keV) after 1100 °C, 10 s annealing.

B. Redistribution

Some typical secondary ion mass spectroscopy (SIMS) plots for Be and Mg as a function of annealing temperature are shown in Fig. 4. For Be there is an apparent defect-assisted diffusion that broadens the profile for 900 °C annealing, but at higher annealing temperatures there is no further motion of the Be. This is similar to the transient-enhanced diffusion seen for implanted B in Si, where there is a rapid, time-dependent motion of the implanted species until the implant damage is annealed. Once this occurs, there is no further defect-assisted diffusion of the implanted species. We find that this situation occurs for Be in GaN, but not for any of the other species, as is clear in the bottom part of Fig. 4 for Mg. At 1450 °C, effective diffusivities of $\leqslant 2\times10^{-13}$ $cm^2\ s^{-1}$ were determined for S, Se, Te, Mg, and C, based on the absence of detectable motion and the spatial resolution of SIMS (~200 Å under these conditions).

C. Residual damage

Figure 5 shows a plan-view TEM and selected-area electron diffraction pattern from a Si-implanted sample (150 keV, 5×10^{15} cm^{-2}) after annealing at 1100 °C for 10 s. This is a high dose implant of the type used for making n^+ ohmic contact regions, and represents a worst-case scenario in terms of damage removal. The sample is still single crystal as determined by the diffraction pattern, but contains a high

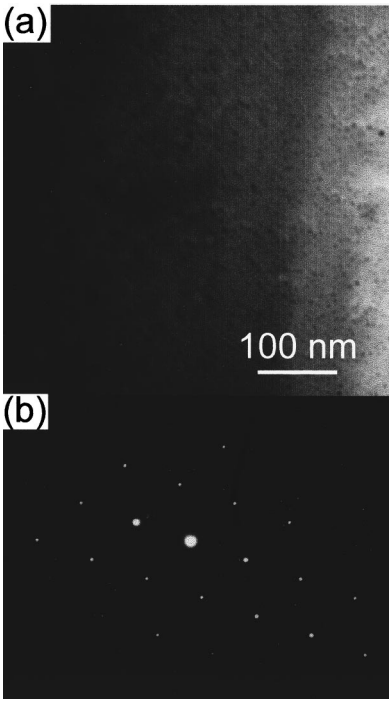

FIG. 6. (a) TEM plan view and (b) selected area diffraction pattern from Si^+-implanted GaN (5×10^{15} cm^{-2}, 150 keV) after 1400 °C, 10 s annealing.

density of extended defects ($\sim10^{10}$ cm^{-2}). This is consistent with past reports of high backscattering yields in implanted GaN annealed at these conditions.[14,15] We ascribe these defects to the formation of dislocation loops in the incompletely repaired lattice.

By sharp contrast, annealing at 1400 °C for 10 s brings a substantial reduction in the implant-induced defects, as shown in Fig. 6. The sample is again single-crystal, but the only contrast in the TEM plan view is due to the lower density ($\sim10^9$ cm^{-2}) of threading dislocations arising from lattice mismatch in the heteroepitaxy. This appears to correlate well with the fact that the highest electron mobility and carrier density in these samples was observed for 1400 °C annealing. Clearly the ultrahigh temperature annealing is required to completely remove lattice damage in GaN implanted with high doses. However, it may not be needed in lower dose material ($\leqslant5\times10^{13}$ cm^{-2}) where the amount of damage created is correspondingly less.

IV. SUMMARY AND CONCLUSIONS

The redistribution and activation of a wide variety of possible donor and acceptor species in GaN was examined. S and Te are found to produce lower room-temperature *n*-type doping levels than Si at the same dose, while only Mg was found to produce *p*-type doping (C- and Be-implanted samples remained *n* type). None of the implanted species showed measurable diffusion at 1450 °C, but Be did display an apparent defect-assisted redistribution at lower temperature (900 °C). For high implant dose (e.g., 5×10^{15} cm^{-2} for Si^+), annealing at 1100 °C is insufficient to remove the lattice damage, while 1400 °C produces much lower defect densities.

ACKNOWLEDGMENTS

The work of R. G. Wilson is partially supported by a grant from ARO. The work at UF is partially supported by a DARPA/EPRI Grant No. MDA 972-98-1-0006 (D. Radack and J. Melcher), and a grant from NSF-DMR (L. Hess), Contract No. 97-32865. Sandia is a multiprogram laboratory operated by Sandia Corporation, a Lockheed-Martin company, for the U.S. Department of Energy under Contract No. DEAC04-94 AL 85000.

[1]J. C. Zolper, J. Cryst. Growth **178**, 175 (1997).
[2]J. C. Zolper, in *GaN and Related Materials, Optoelectronic Properties of Semiconductors and Superlattices* (Gordon and Breach, New York, 1997) Vol. 2.
[3]R. G. Wilson, Proc. Electrochem. Soc. **95-21**, 152 (1995).
[4]H. P. Maruska, M. Lioubtchenko, T. G. Tetreault, M. Osinski, S. J. Pearton, M. Schurman, R. Vaudo, S. Sakai, Q. Chen, and R. J. Shul, Mater. Rev. Soc. Symp. **483**, 345 (1998).
[5]J. C. Zolper, H. H. Tan, J. S. Williams, J. Zou, D. J. H. Cockayne, S. J. Pearton, M. H. Crawford, and R. F. Karlicek, Jr., Appl. Phys. Lett. **70**, 2729 (1997).
[6]S. C. Binari, H. B. Dietrich, G. Kelner, L. B. Rowland, K. Doverspike, and D. K. Wickenden, J. Appl. Phys. **78**, 3008 (1995).
[7]C. Liu, B. Mensching, M. Zeitler, K. Volz, and B. Rauschenbach, Phys. Rev. B **57**, 2530 (1998).
[8]C. Ronning, N. Dalmer, M. Deicher, M. Restle, M. D. Brenser, R. F. Davis, and H. Hofsass, Mater. Res. Soc. Symp. Proc. **468**, 407 (1997).
[9]H. Kobayashi and W. M. Gibson, Appl. Phys. Lett. **73**, 1406 (1998).
[10]T. Suski, J. Jun, M. Leszczynski, H. Teisseyre, I. Grzegopy, S. Porowski, J. M. Baranowski, A. Rockett, S. Strite, A. Stanert, A. Turos, H. H. Tan, J. S. Williams, and C. Jagadish Mater. Res. Soc. Symp. Proc. **482**, 703 (1998).
[11]S. J. Pearton, C. R. Abernathy, C. B. Vartuli, J. C. Zolper, C. Yuan, and R. A. Stall, Appl. Phys. Lett. **68**, 2273 (1996).
[12]J. C. Zolper, R. J. Shul, A. G. Baca, R. G. Wilson, S. J. Pearton, and R. A. Stall, Appl. Phys. Lett. **68**, 2273 (1996).
[13]J. C. Zolper, R. G. Wilson, S. J. Pearton, and R. A. Stall, Appl. Phys. Lett. **68**, 1945 (1996).
[14]J. C. Zolper, J. Han, S. B. Van Deusen, R. M. Biefeld, M. H. Crawford, J. Han, T. Suski, J. M. Baranowski, and S. J. Pearton, Mater. Res. Soc. Symp. Proc. **482**, 609 (1998).
[15]H. H. Tan, J. S. Williams, J. Zou, D. J. H. Cockayne, S. J. Pearton, and R. A. Stall, Appl. Phys. Lett. **69**, 2364 (1996).
[16]J. Burm, K. Chu, W. A. Davis, W. J. Schaff, L. F. Eastman, and T. J. Eustis, Appl. Phys. Lett. **70**, 464 (1997).
[17]J. C. Zolper, J. Han, R. M. Biefeld, S. B. Van Deusen, W. R. Wampler, D. J. Reiger, S. J. Pearton, J. S. Williams, H. H. Tan, and R. Stall, J. Electron. Mater. **27**, 179 (1998).
[18]J. C. Zolper, D. J. Reiger, A. G. Baca, S. J. Pearton, J. W. Lee, and R. A. Stall, Appl. Phys. Lett. **69**, 538 (1996).
[19]M. Fu, V. Sarvepalli, R. K. Singh, C. R. Abernathy, X. A. Cao, S. J. Pearton, and J. A. Sekhar, Mater. Res. Soc. Symp. Proc. **483**, 345 (1998).
[20]X. A. Cao, C. R. Abernathy, R. K. Singh, S. J. Pearton, M. Fu, V. Sarvepalli, J. A. Sekhar, J. C. Zolper, D. J. Rieger, J. Han, T. J. Drummond, R. J. Shul, and R. G. Wilson, Appl. Phys. Lett. **73**, 229 (1998).
[21]M. S. Feng, J. D. Guo, and G. C. Chi, Proc. Electrochem. Soc. **95-21**, 43 (1995).
[22]C. C. Yi and B. W. Wessels, Appl. Phys. Lett. **69**, 3026 (1996).
[23]P. Bogulawski, E. L. Briggs, and J. Bernholc, Phys. Rev. B **51**, 17255 (1995).
[24]C. R. Abernathy, J. D. MacKenzie, S. J. Pearton, and W. S. Hobson, Appl. Phys. Lett. **66**, 1969 (1995).